Cyclin C promotes development and progression of B-cell acute lymphoblastic leukemia by counteracting p53-mediated stress responses

Jana Trifinopoulos,[1] Julia List,[1] Thorsten Klampfl,[1] Klara Klein,[1] Michaela Prchal-Murphy,[1] Agnieszka Witalisz-Siepracka,[1,2] Florian Bellutti,[3] Luca L. Fava,[3] Gerwin Heller,[4] Sarah Stummer,[1] Patricia Testori,[1] Monique L. den Boer,[5,6] Judith M. Boer,[5] Sonja Marinovic,[7] Gregor Hoermann,[8] Wencke Walter,[8] Andreas Villunger,[9] Piotr Sicinski,[10] Veronika Sexl[1,11] and Dagmar Gotthardt[1]

[1]Department for Biological Sciences and Pathobiology, University of Veterinary Medicine Vienna, Vienna, Austria; [2]Department of Pharmacology, Physiology and Microbiology, Division Pharmacology, Karl Landsteiner University of Health Sciences, Krems, Austria; [3]Armenise-Harvard Laboratory of Cell Division, Department of Cellular, Computational and Integrative Biology - CIBIO, University of Trento, Trento, Italy; [4]Division of Oncology, Department of Medicine I, Medical University of Vienna, Vienna, Austria; [5]Princess Máxima Center for Pediatric Oncology, Utrecht, The Netherlands; [6]Erasmus MC-Sophia Children's Hospital, Rotterdam, The Netherlands; [7]Division of Molecular Medicine, Laboratory of Personalized Medicine, Ruder Boskovic Institute, Zagreb, Croatia; [8]MLL Munich Leukemia Laboratory, Munich, Germany; [9]Institute for Developmental Immunology, Biocenter, Medical University of Innsbruck, Innsbruck, Austria; Ludwig Boltzmann Institute for Rare and Undiagnosed Diseases (LBI-RUD), Vienna, Austria; CeMM Research Center for Molecular Medicine of the Austrian Academy of Sciences, Vienna, Austria; [10]Department of Cancer Biology, Dana-Farber Cancer Institute, Boston, MA, USA; Department of Genetics, Blavatnik Institute, Harvard Medical School, Boston, MA, USA and [11]University of Innsbruck, Innsbruck, Austria

Correspondence: D. Gotthardt
dagmar.gotthardt@vetmeduni.ac.at

Received: April 18, 2024.
Accepted: September 30, 2024.
Early view: October 10, 2024.

https://doi.org/10.3324/haematol.2024.285701

Supplementary Information

Cyclin C promotes development and progression of B-cell acute lymphoblastic leukemia by counteracting p53-mediated stress responses

This file includes the Supplementary Figures and Figure Legends, Supplementary Materials and Methods, Supplementary Tables and Supplementary References

Supplementary Figures

Supplementary Figure 1

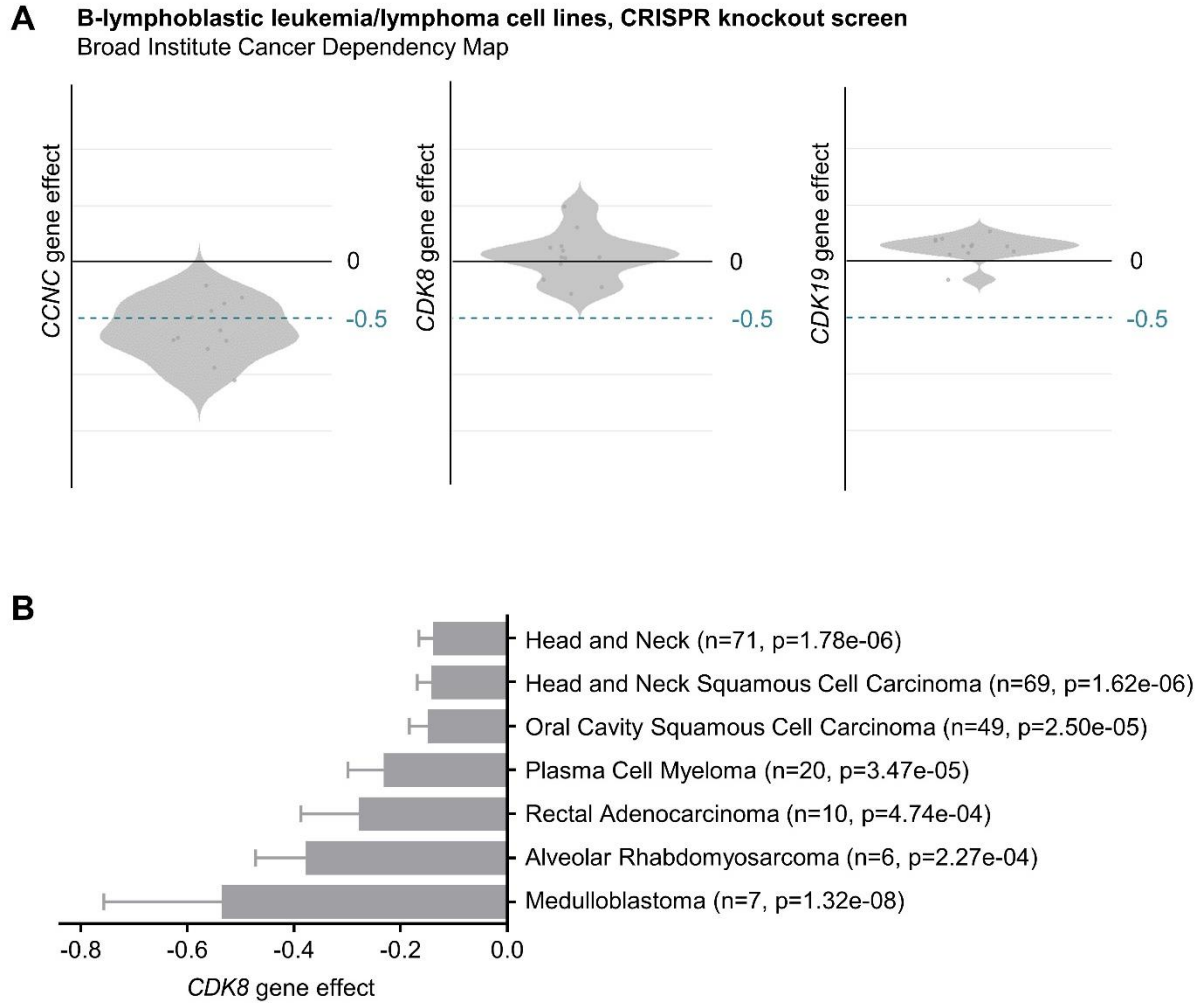

Supplementary Figure 1. (A) CRISPR dependencies for *CCNC*, *CDK8* an *CDK19* as in **Figure 1A**, filtered for cell lines annotated as B-lymphoblastic leukemia/lymphoma (n=12). Dependency score obtained from the Broad Institute Cancer Dependency Map (DepMap Public 23Q2+Score, Chronos). **(B)** Enrichment plot for the top 7 significantly ($p<0.0005$, t-test) enriched lineages based on the Broad Institute Cancer Dependency Map (Depmap) CRISPR dependencies for *CDK8*. The number of cell lines included in each lineage subset is denoted in parentheses and ranking was done based on effect size.

Supplementary Figure 2

A

Genotype	# of animals
Cncfl/fl	273
Cncfl/fl VavCre	241

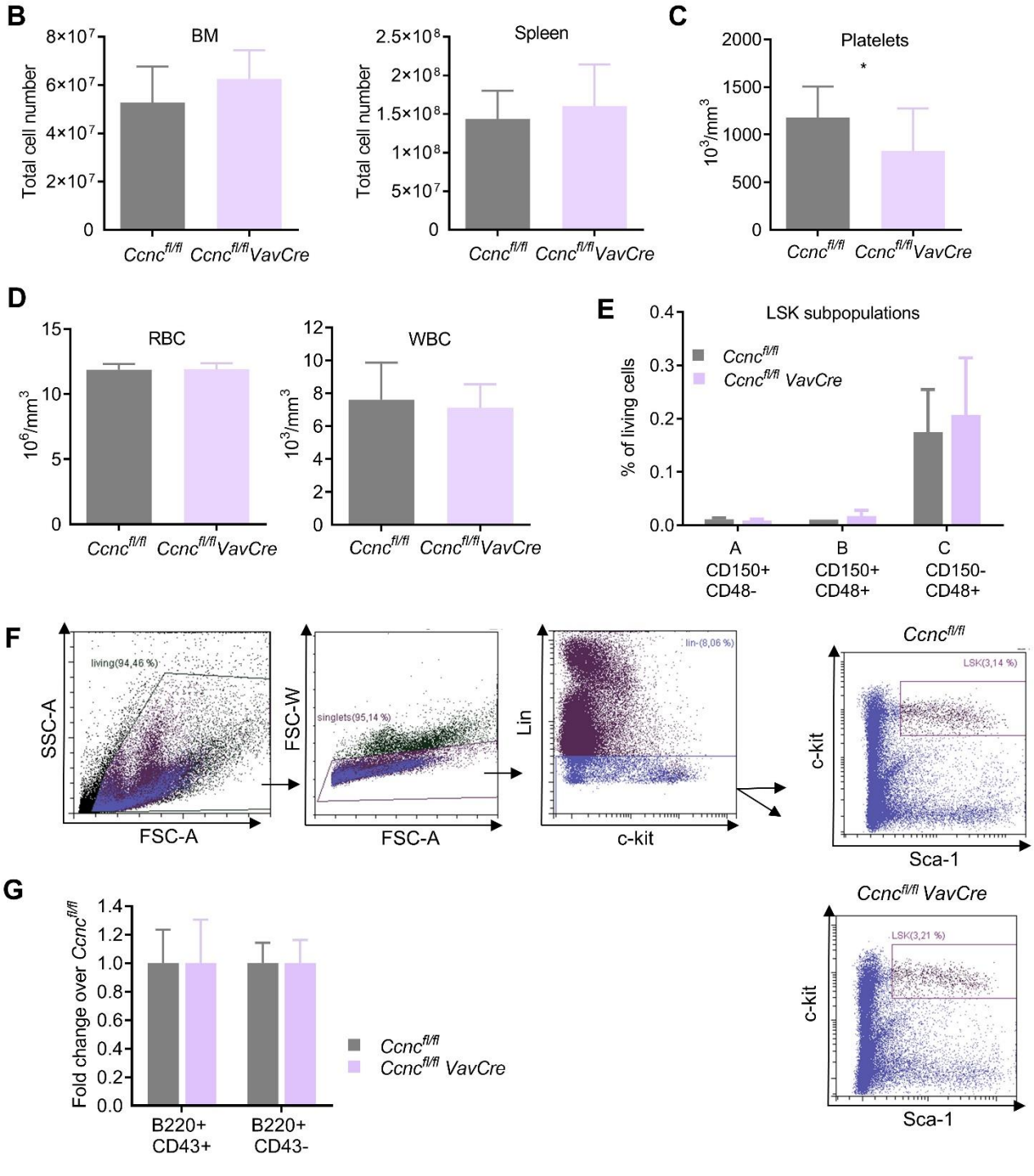

Supplementary Figure 2. (A) Table indicating the genotype of offspring from breedings between *Ccnc*$^{fl/fl}$ *VavCre*$^{-/-}$ *(Ccnc*$^{fl/fl}$*) and Ccnc*$^{fl/fl}$ *VavCre*$^{+/-}$ (*Ccnc*$^{fl/fl}$ *VavCre*) mice (n = 514 offspring, p = 0.158). **(B)** Total counts of living BM (femur and tibia of both hind legs) and splenic cells of *Ccnc*$^{fl/fl}$ and *Ccnc*$^{fl/fl}$ *VavCre* mice (n = 10-12/genotype). **(C)** Platelet count of *Ccnc*$^{fl/fl}$ and *Ccnc*$^{fl/fl}$ *VavCre* mice (n=9-14/genotype), pooled from two independent experiments. **(D)** Analysis of red blood cell count (RBC) and white blood cell count (WBC) of *Ccnc*$^{fl/fl}$ and *Ccnc*$^{fl/fl}$ *VavCre* mice (n=9-14/genotype), pooled from two independent experiments. **(E)** Frequencies of LSK fractions A,B and C in bone marrow of *Ccnc*$^{fl/fl}$ and *Ccnc*$^{fl/fl}$ *VavCre* mice based on expression of CD48 and CD150 (n=10-12/genotype). **(F)** Representative FACS plots for LSK cells in bone marrow of *Ccnc*$^{fl/fl}$ and *Ccnc*$^{fl/fl}$ *VavCre* mice. **(G)** Relative fold change of B220+CD43+/- subpopulations in BM of *Ccnc*$^{fl/fl}$ *VavCre* (n = 10) normalized to the mean value from *Ccnc*$^{fl/fl}$ mice (n = 12). Bar graphs show mean ± SD. Levels of significance were calculated using (A) chi-square test, (B) unpaired t-test or (C, D, E, G) Mann-Whitney U-test. *p < 0.05. Abbreviations: BM, bone marrow; LSK, Lin− Sca-1+ c-kit+

Supplementary Figure 3

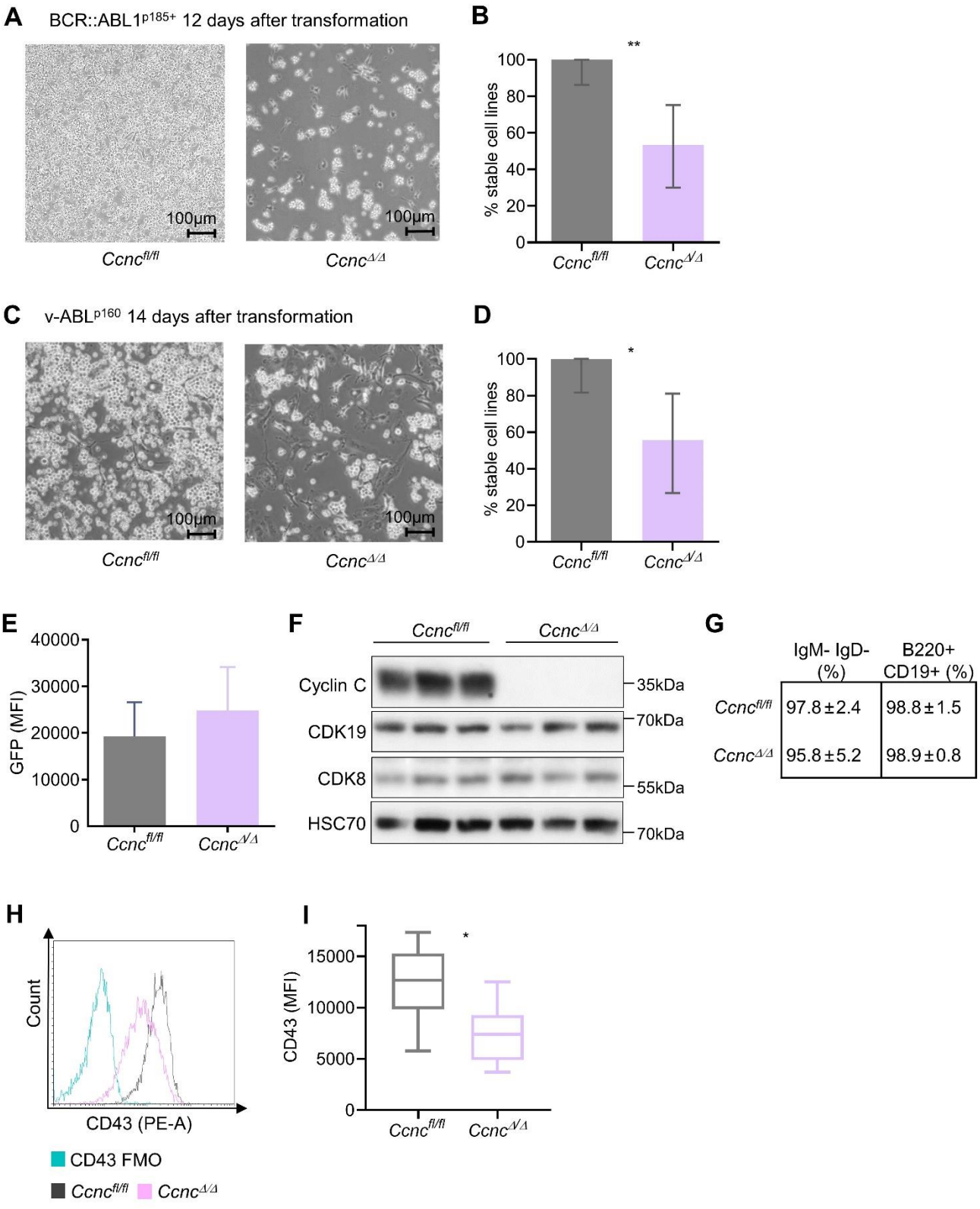

Supplementary Figure 3. (A-D) BM from *Ccnc*$^{fl/fl}$ and *Ccnc*$^{fl/fl}$ *VavCre* mice (n=9/genotype) was transformed with either the *BCR::ABL1*$^{p185+}$ or the *v-ABL*$^{p160+}$ oncogene. Microscopic photographs show representative pictures of cells (A) 12 or (C) 14 days after transformation. Outgrowth of stable cell lines was monitored and outcome summarized in (B) and (D). Error bars represent confidence intervals calculated using the Wilson Score interval (95% confidence level). **(E)** Flow cytometric analysis of GFP expression in stable cell lines established from BM of *Ccnc*$^{fl/fl}$ and *Ccnc*$^{fl/fl}$ *VavCre* mice infected with retrovirus encoding pMSCV-*BCR::ABL1-p185*-IRES-eGFP (n=6-10/genotype). Error bars represent mean ± SD. **(F)** Immunoblotting for levels of cyclin C, CDK8 and CDK19 in stable BCR::ABL1^{p185+} cell lines. HSC70 served as loading control. **(G)** Table indicating frequencies of *Ccnc*$^{fl/fl}$ and *Ccnc*$^{\Delta/\Delta}$ BCR::ABL1^{p185+} cells staining negative for IgM and IgD and double positive for B220 and CD19 (n=7-11/genotype). **(H)** Representative histogram showing CD43 expression of living *Ccnc*$^{fl/fl}$ and *Ccnc*$^{\Delta/\Delta}$ BCR::ABL1^{p185+} cells and **(I)** quantitative analysis (n=7-11/genotype). Center value represents median, the box 25th to 75th percentiles, and whiskers min to max. Levels of significance were calculated using (B,D) Fisher's exact test, (E, G, I) Mann-Whitney U-test. *$p < 0.05$, **$p < 0.01$. Abbreviations: BM, bone marrow; MFI, median fluorescence intensity

Supplementary Figure 4

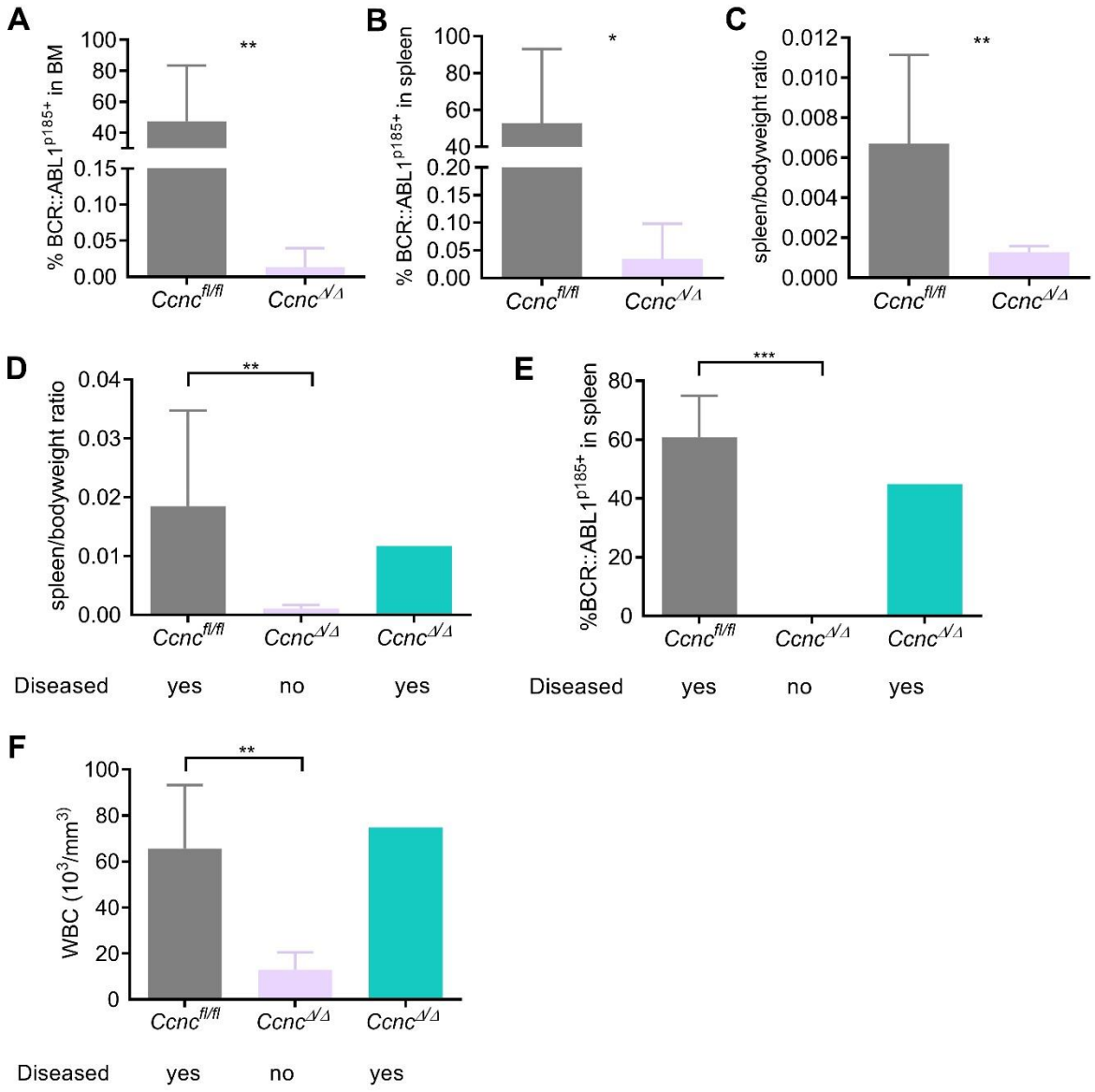

Supplementary Figure 4. (A-C) *Ccnc*$^{fl/fl}$ or *Ccnc*$^{\Delta/\Delta}$ BCR::ABL1^{p185+} cells were intravenously injected into NSG mice and recipient mice were analyzed for disease progression after 26 days (n=9-10 per genotype). **(A)** Infiltration of BCR::ABL1^{p185+-} cells in BM of recipient mice. **(B)** Splenic infiltration of BCR::ABL1^{p185+} cells 26 days after injection. **(C)** Analysis of spleen weights normalized to body weight at day 26 post-injection. **(D-F)** *Ccnc*$^{fl/fl}$ or *Ccnc*$^{\Delta/\Delta}$ BCR::ABL1^{p185+} cells were intravenously injected into NSG mice (n=9-10/genotype) and survival was monitored for up to a maximum of 224-281 days in case of absent disease development. Bar graphs show analysis of diseased mice from *Ccnc*$^{fl/fl}$ cohort compared to mice receiving *Ccnc*$^{\Delta/\Delta}$ BCR::ABL1^{p185+} cell injections of which only one showed disease symptoms. **(D)** Spleen weights normalized to body weight of recipient mice (*Ccnc*$^{fl/fl}$ (n=9), healthy *Ccnc*$^{\Delta/\Delta}$ (n=9), diseased *Ccnc*$^{\Delta/\Delta}$ (n=1)). **(E)** Frequencies of BCR::ABL1^{p185+} cells in spleens of recipient mice (*Ccnc*$^{fl/fl}$ (n=9), healthy *Ccnc*$^{\Delta/\Delta}$ (n=5), diseased *Ccnc*$^{\Delta/\Delta}$ (n=1)). **(F)** White blood cell count (WBC) in mice receiving *Ccnc*$^{fl/fl}$ BCR::ABL1^{p185+} injections compared with *Ccnc*$^{\Delta/\Delta}$ cohort (*Ccnc*$^{fl/fl}$ (n=5), healthy *Ccnc*$^{\Delta/\Delta}$ (n=4), diseased *Ccnc*$^{\Delta/\Delta}$ (n=1)). Graphs show mean ± SD. Mann-Whitney U-test (A, B, E) or unpaired t-test (C, D, F) were used to calculate levels of significance. *p < 0.05, **p < 0.01, ***p < 0.001. Abbreviations: BM, bone marrow

Supplementary Figure 5

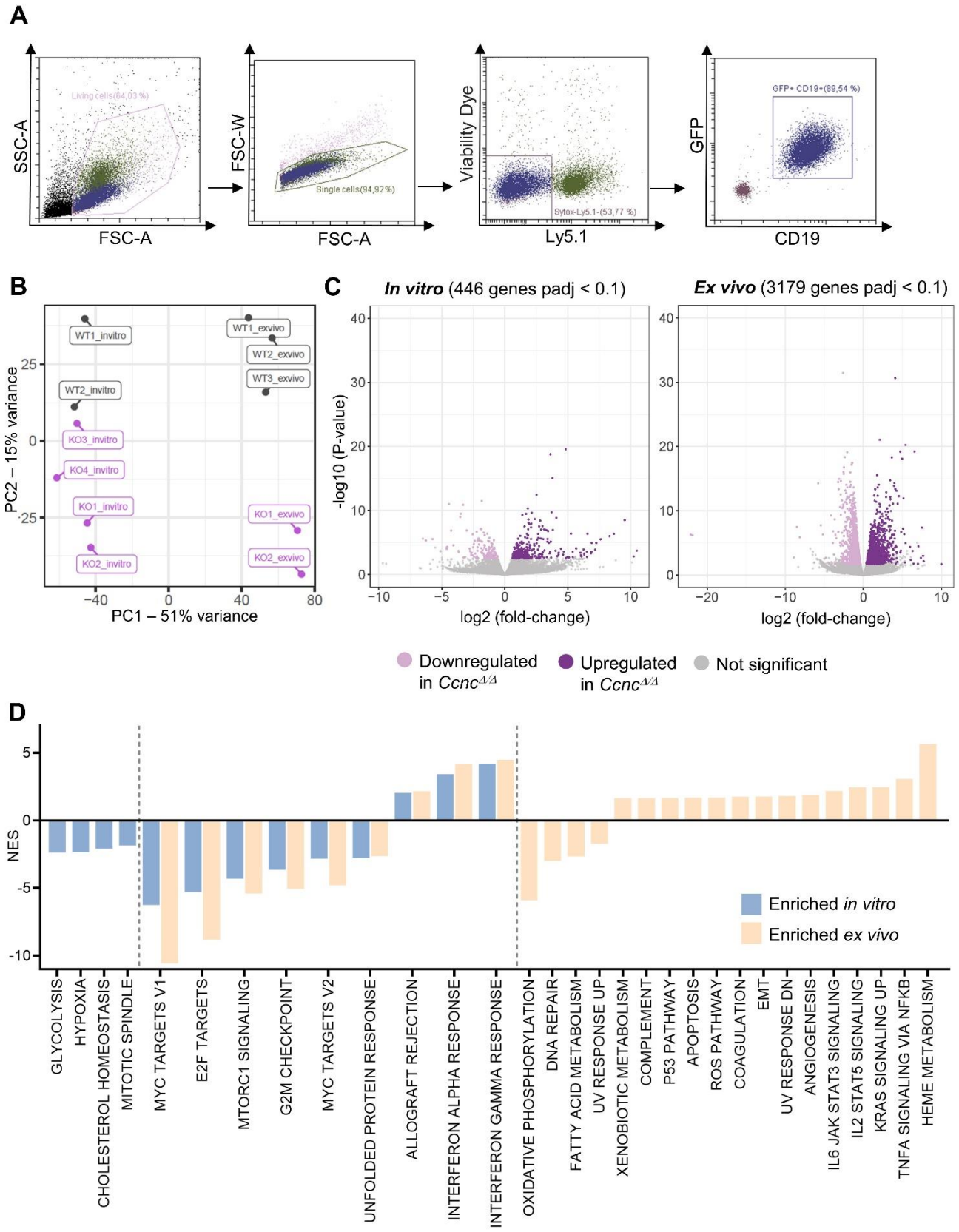

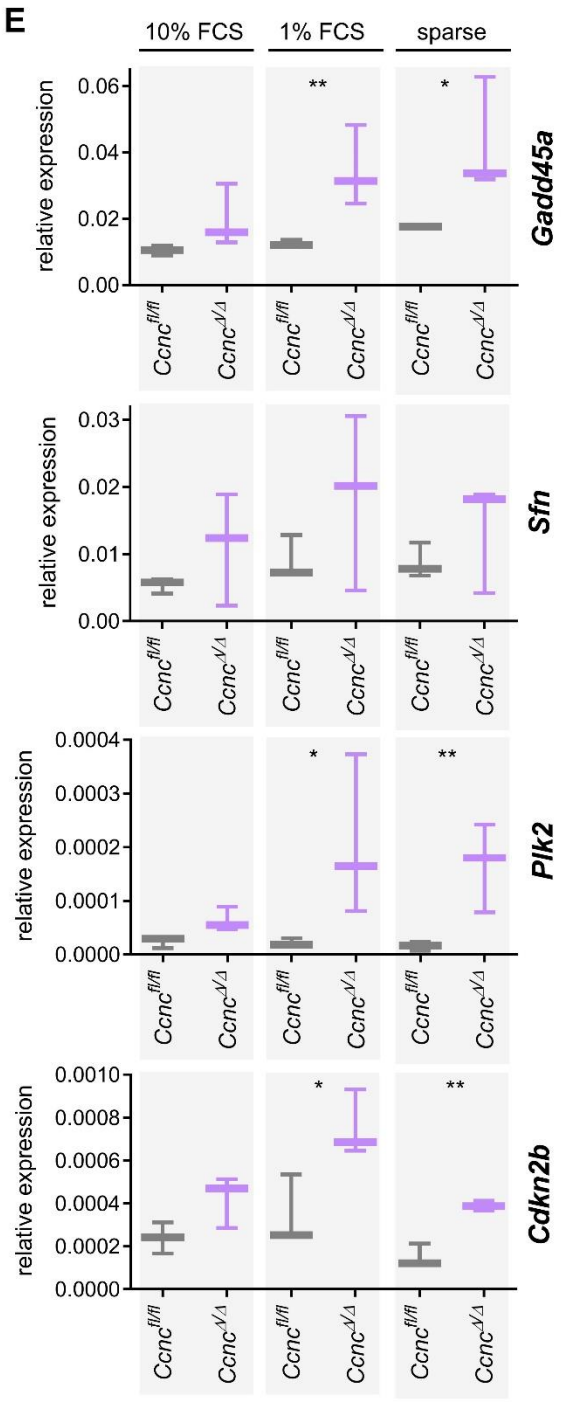
E
10% FCS
1% FCS
sparse
relative expression
Gadd45a
Sfn
Plk2
Cdkn2b
Ccnc^fl/fl
Ccnc^Δ/Δ

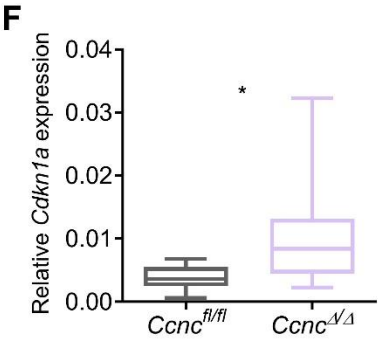
F
Relative Cdkn1a expression
Ccnc^fl/fl
Ccnc^Δ/Δ

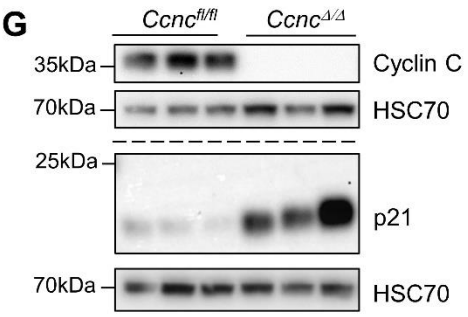
G
Ccnc^fl/fl
Ccnc^Δ/Δ
35kDa
Cyclin C
70kDa
HSC70
25kDa
p21
70kDa
HSC70

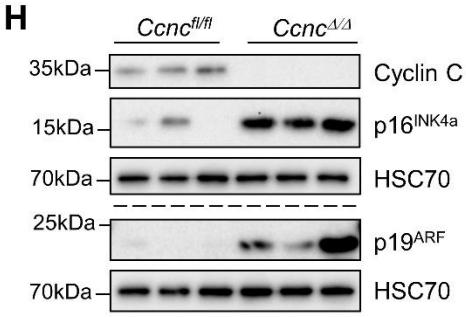
H
Ccnc^fl/fl
Ccnc^Δ/Δ
35kDa
Cyclin C
15kDa
p16INK4a
70kDa
HSC70
25kDa
p19ARF
70kDa
HSC70

Supplementary Figure 5. (A) Representative flow cytometric plots showing the gating strategy for retrieval of BCR::ABL1^{p185+} cells from BM of inoculated NSG mice. Ten days after intravenous injection of NSG mice with BCR::ABL1^{p185+} cells, living Ly5.1^{-}CD19^{+}GFP^{+} cells were sorted and used for subsequent RNA-Seq analyses (*ex vivo* samples). **(B**) Principal Component Analysis (PCA) of stable *Ccnc*$^{fl/fl}$ (WT) and *Ccnc*$^{\Delta/\Delta}$(KO) BCR::ABL1^{p185+} cell lines before (*in vitro*) and after injection into NSG mice (*ex vivo*, retrieved from BM 10 days post-injection). **(C)** Volcano plots of differentially expressed genes (padj <0.1) in *Ccnc*$^{\Delta/\Delta}$ BCR::ABL1^{p185+} vs. *Ccnc*$^{fl/fl}$ BCR::ABL1^{p185+} cells before injection into NSG mice (*in vitro*, left) and after retrieval from BM of recipient mice (*ex vivo*, right). **(D)** GSEA results showing significantly (|NES| >1, FDR <0.2, p<0.05) enriched hallmark gene sets in *Ccnc*$^{\Delta/\Delta}$BCR::ABL1^{p185+} vs. *Ccnc*$^{fl/fl}$ BCR::ABL1^{p185+} cells. Gene sets only enriched *in vitro* are shown on the left, commonly enriched gene sets in the middle, and gene sets uniquely enriched in *ex vivo* samples are depicted on the right. **(E)** Expression of genes that contributed to core enrichment of the hallmark p53 pathway gene set in *ex vivo* derived *Ccnc*$^{\Delta/\Delta}$ BCR::ABL1^{p185+} cells were evaluated via RT-qPCR of RNA extracted from *in vitro* cultured *Ccnc*$^{fl/fl}$ and *Ccnc*$^{\Delta/\Delta}$ BCR::ABL1^{p185+} cells in different conditions (cells cultured in standard medium supplemented with 10% FCS (left panel), with reduced FCS (1%, middle panel) and with reduced cell density (right panel)). Expression levels were normalized to *Actb.* Experiment was performed in technical duplicates of n=3 independent cell lines/genotype. Center value represents median, the box 25th to 75th percentiles, and whiskers min to max. **(F)** Expression of *Cdkn1a* relative to *Rplp0* of *Ccnc*$^{fl/fl}$ (n=10) and *Ccnc*$^{\Delta/\Delta}$ BCR::ABL1^{p185+} (n=8) cell lines from two independent qRT-PCR experiments performed in technical duplicates. Center values represent median of biological replicates, the box 25th to 75th percentiles, and whiskers min to max. **(G)** Analysis of cyclin C and p21 protein levels on two separate immunoblots showing the same *Ccnc*$^{fl/fl}$ versus *Ccnc*$^{\Delta/\Delta}$ BCR::ABL1^{p185} cell line lysates (n=3 independent cell lines per genotype). HSC70 served as loading control. **(H)** Immunoblot analysis of p16^{INK4a} and p19^{ARF} levels in *Ccnc*$^{fl/fl}$ versus *Ccnc*$^{\Delta/\Delta}$ BCR::ABL1^{p185} cells (n=3 biological replicates per genotype). Analysis was performed on two separate immunoblots with the same lysates, HSC70 was used as loading control. Levels of significance (E,F) were calculated using unpaired t-test on ΔCt values. *p < 0.05, **p < 0.01. Abbreviations: RNA-Seq, RNA sequencing; BM, bone marrow; PC, principal component; padj, Benjamini-Hochberg adjusted p-value; GSEA, gene set enrichment analysis; EMT, epithelial–mesenchymal transition; ROS, reactive oxygen species; NES, normalized enrichment score; FDR, false discovery rate; RT-qPCR, real-time quantitative PCR; FCS, fetal calf serum

Supplementary Figure 6

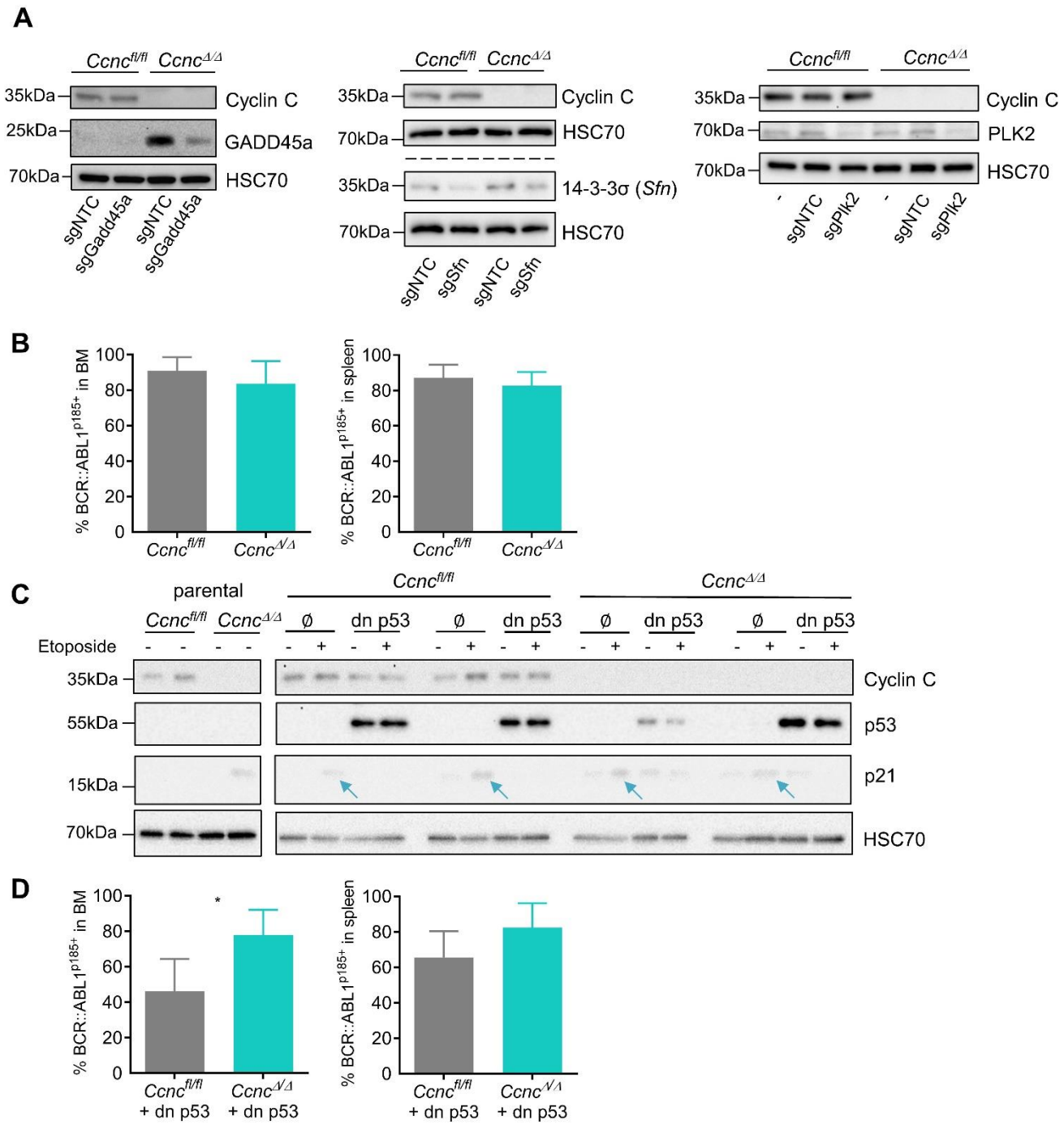

Supplementary Figure 6. (A) Immunoblot analysis showing levels of GADD45a, 14-3-3σ (encoded by *Sfn*) and PLK2 after CRISPR/Cas9 mediated targeting of the respective genes in stable *Ccnc*$^{fl/fl}$ and *Ccnc*$^{\Delta/\Delta}$ BCR::ABL1^{p185+} cell lines in standard culture medium supplemented with 10% FCS. Non-targeting control (sgNTC) or mock treated cells (-) served as control. HSC70 was used as loading control. **(B)** *Ccnc*$^{fl/fl}$ or *Ccnc*$^{\Delta/\Delta}$ BCR::ABL1^{p185+} cells with spontaneous p53 mutations were intravenously injected into NSG mice and survival was monitored. Bar graphs show flow cytometric analysis of BM and spleen infiltration of diseased mice (n = 4 per genotype). **(C)** Cyclin C, p53 and p21 immunoblot analysis of *Ccnc*$^{fl/fl}$ and *Ccnc*$^{\Delta/\Delta}$ BCR::ABL1^{p185+} cell lines infected with dominant negative p53 (dn p53) or empty vector (∅). Cells were treated with DMSO as control or etoposide (1 µmol/L) for 4 hours to induce p53-dependent p21 expression. HSC70 was used as loading control (n=2 independent cell lines/genotype). **(D)** *Ccnc*$^{fl/fl}$ + dn p53 or *Ccnc*$^{\Delta/\Delta}$ + dn p53 BCR::ABL1^{p185+} cells were intravenously injected into NSG mice and survival was monitored. Bar graph shows infiltration of BCR::ABL1^{p185+} cells in BM and spleens of diseased mice assessed by flow cytometry (n=5 per genotype). Error bars show mean ± SD. Mann-Whitney U-test was used to calculate levels of significance (B,D). *$p < 0.05$. Abbreviations: BM, bone marrow; FCS, fetal calf serum

Supplementary Figure 7

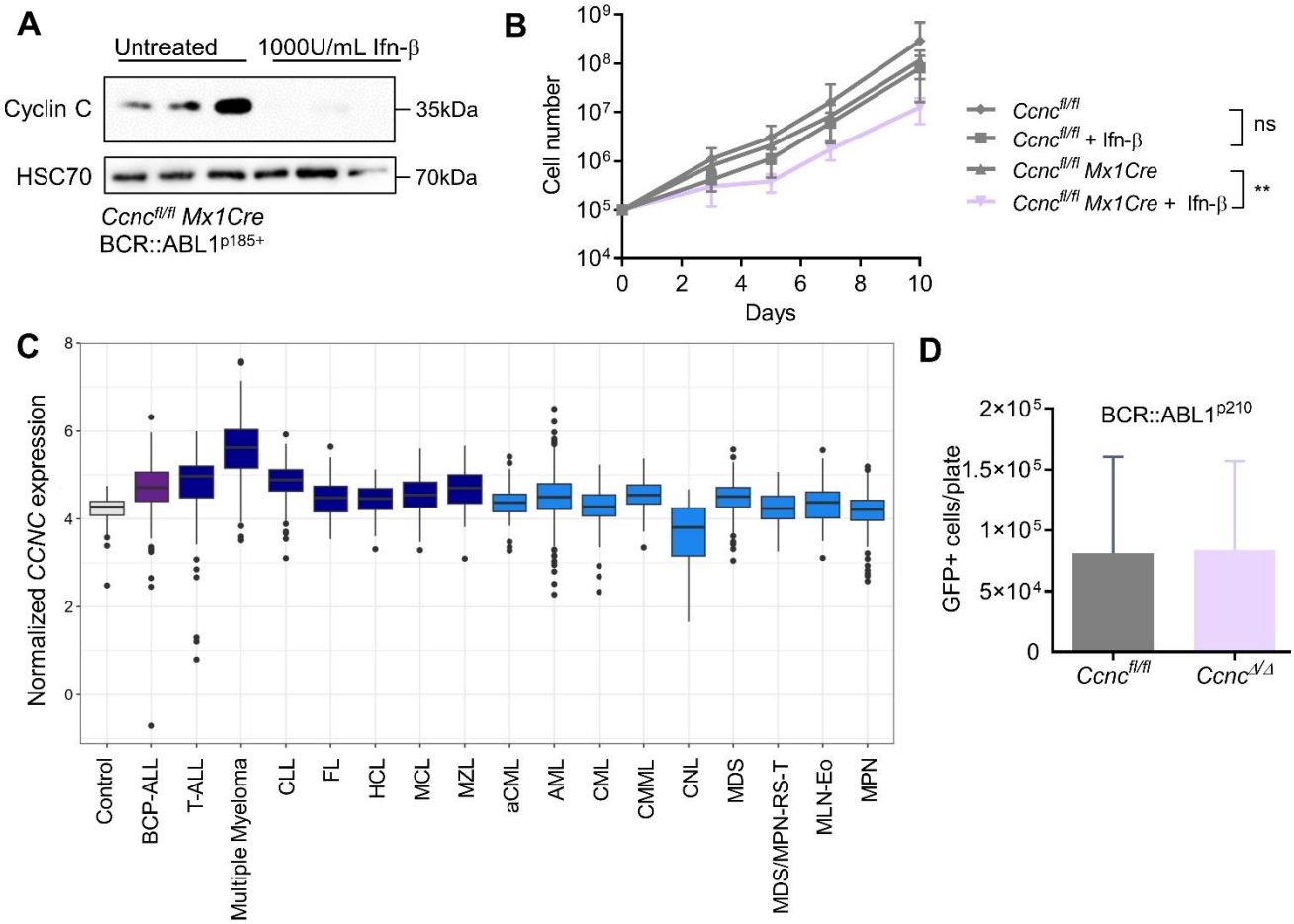

Supplementary Figure 7. (A) Immunoblot analysis verifying cyclin C deletion in *Ccnc*$^{fl/fl}$ *Mx1Cre* BCR::ABL1^{p185+} cells after treatment with 1000U/mL Ifn-β. HSC70 served as loading control (n=3 independent cell lines per genotype). **(B)** *Ccnc*$^{fl/fl}$ *Mx1Cre* (n=4) cell lines were treated with Ifn-β (1000U/mL) and proliferation was assessed for 10 days. As control, equally treated *Ccnc*$^{fl/fl}$ (n=6) cell lines as well as untreated cell lines (n=4-6/genotype) were used. **(C)** *CCNC* gene expression profile in control (BM mononuclear cells, n=64) vs. patient samples (B-cell precursor acute lymphoblastic leukemia (BCP-ALL): n = 321; T-ALL: n = 136; multiple myeloma: n = 261; chronic lymphocytic leukaemia (CLL): n = 278; follicular lymphoma (FL): n = 63; hairy cell leukemia (HCL), n = 74; mantle cell lymphoma (MCL): n = 83; marginal zone lymphoma (MZL): n= 81; atypical chronic myeloid leukemia (aCML): n = 78; acute myeloid leukemia (AML): n = 743; chronic myeloid leukemia (CML): n = 119; chronic myelomonocytic leukemia (CMML): n = 225; chronic neutrophilic leukemia (CNL): n = 33; myelodysplastic syndrome (MDS): n = 751; MDS/myeloproliferative neoplasm (MPN) with ring sideroblasts and thrombocytosis (MDS/MPN-RS-T): n = 111; myeloid or lymphoid neoplasms associated with eosinophilia (MLN-Eo): n = 46; MPN: n = 259). **(D)** BM from *Ccnc*$^{fl/fl}$ and *Ccnc*$^{fl/fl}$ *VavCre* mice was isolated and infected with a retrovirus encoding the *BCR::ABL1*^{p210} oncogene prior to plating in growth-factor free methylcellulose. The number of GFP^{+} cells/plate was determined via flow cytometry after 17 days (n=4/genotype, performed in technical duplicates, one representative result out of two is shown). Error bars depict mean ± SD. Statistical significance was calculated using (B) unpaired t-test on log-transformed counts from day 10 or (D) Mann-Whitney U-test. **p < 0.01. Abbreviations: Ifn-β, interferon beta; BM, bone marrow

Supplementary Materials and Methods

Cell culture maintenance and growth curves

BCR::ABL1^{p185+} cell lines were maintained in RPMI-1640 (Sigma) medium supplemented with 10% fetal bovine serum (FBS; Bio & Sell), 100U/mL penicillin, 100µg/mL streptomycin and 50µM β-mercaptoethanol (Sigma) (RPMI complete medium). The NALM-6 (RRID:CVCL_0092) cell line was kindly provided by Luca Fava (University of Trento, Italy) and cultured in RPMI complete medium supplemented with 10% heat-inactivated FBS. Phoenix-Eco (RRID:CVCL_H717) and A010 Ab-MuLV producer cells were maintained in Dulbecco's Modified Eagle's Medium (DMEM; Sigma) with 10% FBS, 100U/mL penicillin and 100µg/mL streptomycin. For BCR::ABL1^{p185+} growth curves, cells were plated at a density of 10^5 cells/mL in medium supplemented with 10%FBS. To assess proliferation under stress, cells were seeded with reduced serum (10^5 cells/mL, 1%FBS) or at a reduced cell density (10^4/mL, 10%FBS). Cell lines were cultured at 37 °C with 5% CO_2 and regularly tested negative for mycoplasma.

Western Blot analysis

Protein lysates were prepared using SDS lysis buffer or Laemmli lysis buffer. Equal amounts of protein were separated on an 8, 10 or 12% SDS-PAGE gel and transferred to nitrocellulose membranes (Amersham Protran, Merck) or PVDF membranes (Immobilon-P, Merck Millipore) via overnight blotting (0.2mA for 18h followed by 0.4mA for 5h at 4°C) or using a Trans-Blot Turbo System (Bio-Rad). After probing with primary antibodies and incubation with the secondary antibodies (**Supplementary Table S3**), immunoreactive bands were visualized using Clarity Western ECL substrate (BioRad) and the ChemiDoc Touch Imaging System (BioRad).

PCR and qRT-PCR analyses

For comparison of stress responses, BCR::ABL1^{p185+} cells were plated at a density of 10^5 cells/mL in medium supplemented with 10%FBS. To elicit a stress response, the concentration of FBS was either reduced (1% FCS) or cells were plated at a reduced density (10^4 cells/mL) for 48 hours prior to RNA isolation. RNA was isolated using the RNeasy Mini Kit (QIAGEN) and reverse transcription was performed using the iScript cDNA Synthesis Kit (Bio-Rad) according to the manufacturer's instructions. The real-time quantitative PCRs (RT-qPCR) were performed using the SsoAdvanced Universal SYBR Green Supermix (Bio-Rad) following the manufacturer's instructions on a CFX96 real-time PCR detection system (Bio-Rad). The qRT-PCR primer sequences are listed in **Supplementary Table S4**. To assess the p53 mutational status, the *Tp53* coding sequence was amplified and Sanger sequenced as previously described[1].

Hemocytometry, histology and microscopy

Blood was collected into EDTA tubes (Mini-Collect K3EDTA Tubes, Greiner Bio-One) from the *vena facialis*. White blood cell (WBC), red blood cell (RBC) and platelet counts were measured using an animal blood counter (scil Vet abc). Blood smears were stained with the Hemacolor Rapid staining of blood smears kit (Sigma-Aldrich). For microscopic images, an Olympus IX71 microscope and the cellSens Dimension software (Olympus) were used.

Flow cytometry and cell sorting

For flow cytometric analysis of primary murine material, single cell suspensions were prepared from bone marrow (BM) and spleen. Blood was collected via puncturing the *vena facialis* and erythrocyte lysis was performed using either red blood cell lysis buffer (10 mM KHCO3 and 75 mM NH4Cl, pH 7.4) or BD FACS Lysing Solution (BD Bioscience). The list of antibodies can be found in **Supplementary Table S2**.

Hematopoietic populations were defined as follows: CLP ($Lin^-CD127^+c\text{-}kit^{mid}Sca\text{-}1^{mid}$ $CD127^+$); HSC ($CD150^+CD48^-CD135^-CD34^-$), MPP1 ($CD150^+CD48^-CD135^-CD34^+$), MPP2 ($CD150^+CD48^+CD135^-$ $CD34^+$), MPP3 ($CD150^-CD48^+CD135^-$), and MPP4 ($CD150^-CD48^+CD135^+$) cell populations gated on $Lin^-Sca\text{-}1^+c\text{-}kit^+$ (LSK) cells. For exclusion of Lin^+ cells, BM was stained with lineage markers (B220, TER119, CD3, Gr-1 and Mac-1). B-cell development populations were defined according to Basel (Hardy/Philadelphia) nomenclature in pre-pro B cells ($B220^+CD43^+CD19^-BP\text{-}1^-$, fraction A), pro-B ($B220^+CD43^+CD19^+BP\text{-}1^-$, fraction B), pre-BI/large pre-BII ($B220^+CD43^+CD19^+BP\text{-}1^+$, fraction C/C'), small pre-BII ($B220^+CD43^-IgM^-IgD^-$, fraction D), immature B cells ($B220^+CD43^-$ IgM^+IgD^-, fraction E), and mature B cells ($B220^+CD43^-IgM^+IgD^+$, fraction F)[2–4].

Apoptosis stainings were performed using the Annexin V Apoptosis Detection Kit (eFluor 450, 7-AAD) (ThermoFisher) according to manufacturer's instructions. Cell cycle analysis was performed by staining cells for 30 minutes at 37°C with propidium iodide (PI) staining buffer (0.1% sodium citrate, 0.1% Triton X-100, 100 µg/mL RNAse, 20 µg/mL PI). As viability dye, SYTOX Blue Dead Cell Stain (ThermoFisher) was used.

Flow cytometric experiments were performed on a CytoFLEX or CytoFLEX S flow cytometer (Beckman Coulter) and cells were sorted on a BD FACSAria III (BD Bioscience). Data were analysed using CytExpert (version 2.4).

Mouse strains

Conditional *Ccnc*$^{fl/fl}$ mice were kindly provided by Piotr Sicinski[5] and bred to *VavCre*[6] and *Mx1Cre*[7] mice. NSG (NOD.Cg-*Prkdc*^{scid} *Il2rg*tm^{1Wjl}/SzJ; Charles River), *Ccnc*$^{fl/fl}$ *VavCre* (mixed, *C57BL/6N* × *Sv129*) and *Ccnc*$^{fl/fl}$ *Mx1Cre* (*C57BL/6N*) mice were bred and maintained under pathogen-free conditions at the University of Veterinary Medicine Vienna, Austria, according to Federation for Laboratory Animal Science Associations (FELASA) guidelines.

Retroviral transductions and establishment of leukemic cell lines

For transformation with the *BCR::ABL1*$^{p185+}$ fusion gene the Phoenix ecotropic packaging system (Phoenix-Eco) and a pMSCV-IRES-GFP retroviral vector containing the *BCR::ABL1*$^{p185+}$ oncogene were used. Briefly, plasmid DNA diluted in serum-free DMEM supplemented with TurboFect (Thermo Fisher Scientific) and 10mM HEPES buffer (pH 7.4) was incubated at room temperature for 15 minutes before dropwise addition to Phoenix-Eco cells (~70% confluency). After incubation for 24 hours at 37°C in a CO_2 incubator, the medium was replaced by the RPMI target cell medium. This viral supernatant was collected 24 and 48 hours later, filtered (0.45µm) and supplemented with 4µg/mL polybrene (Sigma) as well as 10ng/mL interleukin 7 (IL-7; R&D) to infect freshly isolated BM from *Ccnc*$^{fl/fl}$, *Ccnc*$^{fl/fl}$ *VavCre* or *Ccnc*$^{fl/fl}$ *Mx1Cre* mice. To generate stable BCR::ABL1^{p185+} cell lines, cells were then maintained in RPMI complete medium and monitored for outgrowth. Flow cytometric stainings confirmed all outgrowing *Ccnc*$^{fl/fl}$ and *Ccnc*$^{\Delta/\Delta}$ BCR::ABL1^{p185+} cell lines as B220+CD19+IgM-IgD- pro-B cells which did not express other lineage markers. An analogous procedure was used for the generation of BCR::ABL1^{p185+} cell lines carrying a dominant negative p53 (dn p53) variant by retrovirally infecting stable BCR::ABL1^{p185+} cell lines with a pMSCV-dn-p53-IRES-GFP vector or empty vector as control[8,9]. For *in vitro* deletion of cyclin C in BCR::ABL1^{p185+} *Ccnc*$^{fl/fl}$ *Mx1Cre* cell lines, 1000U/mL recombinant mouse interferon-β (IFN-β; Sigma) was added to the cells for 48 hours. Untreated cells and BCR::ABL1^{p185+} *Ccnc*$^{fl/fl}$ cells were used as controls. To generate v-abl^{p160+} cell lines, viral supernatant from A010 Ab-MuLV producer cells was harvested, filtered (0.45µm) and supplemented with 4µg/mL polybrene and 10µg/mL IL-7 before infecting *Ccnc*$^{fl/fl}$ and *Ccnc*$^{fl/fl}$ *VavCre* BM.

Colony formation assays

For colony formation assays, BM from gender- and age-matched 6-10 week old *Ccnc*$^{fl/fl}$ or *Ccnc*$^{fl/fl}$ *VavCre* mice was retrovirally transduced with the *BCR::ABL1*^{p185} oncogene as detailed above. For transformation with the *BCR::ABL1*^{p210} fusion gene, a retroviral producer cell line based on the gpE+86 system was used as previously described[10]. As control, BM cells were seeded in complete medium. After 24 hours, cells were washed, and equal numbers were seeded in methylcellulose (mouse

methylcellulose base media, R&D Systems) without additional supplements. Another 14-18 days later, colonies were counted and photographed. Cells from BCR::ABL1^{p210+} plates were harvested, washed and counted via FACS. Representative BCR::ABL1^{p185+} colonies were picked, washed, and seeded in RPMI complete medium to monitor outgrowth in liquid culture. For IL-7 dependent colony growth, single cell suspensions were prepared from BM of *Ccnc$^{fl/fl}$* or *Ccnc$^{fl/fl}$ VavCre* mice. The cells were washed, counted and equal numbers embedded in methylcellulose containing 10ng/mL IL-7 (R&D).

RNA Sequencing of BCR::ABL1^{p185+} cell lines

In vitro samples for RNA sequencing were prepared from stable *Ccnc$^{fl/fl}$* or *Ccnc$^{fl/fl}$ VavCre* BCR::ABL1^{p185+} cell lines (n=4). *Ex vivo* samples were generated by injecting the same cell lines into gender-matched, 11 week old NSG mice ($5x10^5$ cells injected i.v. via tail vein). For retrieval of BCR::ABL1^{p185+} cells ten days after injection, living (Sytox Blue-negative) Ly5.1$^-$CD19$^+$GFP$^+$ cells were sorted. A total of $4x10^5$-$1x10^6$ *Ccnc$^{fl/fl}$* BCR::ABL1^{p185+} cells and $2.2x10^5$ *Ccnc$^{\Delta/\Delta}$* were sorted from the BM. Total RNA was extracted using the RNeasy Micro Kit (QIAGEN). The RNA was subjected to library prep for next generation sequencing (NGS) with Illumina technology using the SmartSeq3 protocol[11] and Nextera adapters. Sequencing was performed on an Illumina NovaSeq Instrument (Illumina, San Diego, CA, USA), using an S4 flowcell with paired-end mode, sequencing 150 bp per read. Raw reads were quality controlled using Fastqc version 0.11.9. Trimmomatic version 0.39[12] was used to filter reads and umi-tools version 1.1.1[13] was used to remove unique molecular identifier sequences. The reads were then aligned against the GRCm38 primary assembly mouse reference genome using STAR version 2.7.6a with the "Gencode M25 primary assembly annotation" gene model[14,15]. Reads covering exons were counted using the featureCounts program[16] from the Subread package version 2.0.1[17] and total counts were reported at the gene level for each sample in form of a count matrix. Further quality control by assessing fraction of reads assigned to genes, by comparison of count distributions and by principal component analysis identified 5/16 samples to be of low quality. These samples were excluded from further analysis. Differential gene expression was analyzed with R version 4.0.3 using RStudio version 1.3.1093 and the DESeq2 package version 1.30.0[18–20]. The RNA-Seq data reported in this article have been deposited in the Array Express database (accession number: E-MTAB-13728).

Gene set enrichment analysis (GSEA)

For GSEA, ranked gene lists were prepared from the results of the differential gene expression analysis[21,22]. We used sign(log2FoldChange) * (-1) * log10(p-value) as the rank metric for each gene ("log2FoldChange" and "p-value" were taken from the DESeq2 results object). GSEA was then performed using the GSEA software (version 4.1.0). Enrichment of gene set collections from MSigDB

(version 7.2) was tested[23,24]. The analysis was performed using the command-line script and the "GSEAPreranked" analysis mode. To map mouse ensembl gene IDs to human gene symbols we used the gene annotation chip-file provided with MSigDB after removal of duplicate mappings. The "collapse" parameter was set to "Remap_Only" and the "scoring_scheme" parameter to "classic".

DepMap Analysis

Genetic dependency analyses in a panel of tumor cell lines were performed using the DepMap platform (https://depmap.org/portal/, accessed on 8.11.2023) and the most recent DepMap CRISPR database (Depmap Public 23Q2+Score, Chronos)[25–28].

CRISPR/Cas9 mediated knock-out cell lines

Knock-out NALM-6 cells were generated using direct delivery of the CRISPR/Cas9 system as previously described[29] with a ribonucleoprotein (RNP) complex consisting of Cas9 protein and guide RNAs (gRNAs) targeting *HPRT1* (GCATTTCTCAGTCCTAAACA) or one of three guides targeting *CCNC* (TAGGCAAAGATCCGTTCTGT, GGCCCATGTCCTGCACATAC and TCTGTTGAAGGAGCGCCAAA). Briefly, crRNA (100µM, IDT) and tracrRNA (100µM, IDT) were annealed in equimolar concentrations to form gRNAs. For a total of $2x10^5$ NALM-6 cells, 120pmol recombinant Cas9 (IDT) were complexed with 150pmol of the respective gRNA for RNP formation. Electroporation was performed using Lonza Nucleofector 4D according to manufacturer's instructions and 4µM electroporation enhancer (100µM, IDT). Monoclonal cell lines were generated in 96-well plates through limiting dilution, or by seeding single cells with a BD FACSAria III (BD Bioscience) cell sorter. An analogous procedure was used for CRISPR/Cas9 mediated gene editing in BCR::ABL1^{p185+} cell lines using Lonza Nucleofector 2b with 1µM electroporation enhancer and $1x10^6$ cells. Two different gRNAs per gene were pooled to target *Gadd45a* (CTCGTACACGCCGACCGTAA, GGCACAGTACCACGTTATCG), *Sfn* (GTAGCTTACAAGAACGTGGT, TTCCGTAGCTTACAAGAACG) or *Plk2* (TTATAGTCGACCCCACGACG, ACGAACAAGAAATCTTGCAC). Assays were performed 6 days after direct delivery of the respective RNP complex.

Data Visualization and Statistical Analysis

Data were visualized and analyzed using R version 4.3.2[18] with RStudio version 2023.09.1[19] or GraphPad Prism version 8.4.3 for Windows (GraphPad Software, San Diego, California USA, www.graphpad.com). Statistical significance was calculated using the appropriate statistical method as indicated in the corresponding Figure Legends. CorelDRAW Graphics Suite (version 23.0.0.363) was used for some graphical illustrations.

Supplementary Tables

Supplementary Table S1. Differentially expressed p53 hallmark genes.

Differentially expressed genes (padj<0.1) in the p53 hallmark mouse gene set[21,23,24,30,31] between *Ccnc*$^{\Delta/\Delta}$ vs. *Ccnc*$^{fl/fl}$ BCR::ABL1^{p185+} cells after retrieval from BM of NSG mice ("*ex vivo*" samples) 10 days post-injection, sorted by log2 fold-change.

Gene	ID	log2 (fold-change)	padj
Ptpn14	ENSMUSG00000026604.17	5.09	3.54E-06
Cdkn2a	ENSMUSG00000044303.6	2.89	6.45E-02
Ndrg1	ENSMUSG00000005125.13	2.88	5.14E-03
Rgs16	ENSMUSG00000026475.7	2.33	7.26E-04
Ier3	ENSMUSG00000003541.6	1.95	6.49E-02
Cdkn2b	ENSMUSG00000073802.5	1.92	1.42E-03
Stom	ENSMUSG00000026880.11	1.87	1.10E-02
Tcn2	ENSMUSG00000020432.12	1.82	1.07E-02
Gadd45a	ENSMUSG00000036390.8	1.78	2.85E-03
Btg1	ENSMUSG00000036478.8	1.74	1.11E-08
Plk2	ENSMUSG00000021701.8	1.74	3.57E-02
Pitpnc1	ENSMUSG00000040430.18	1.39	8.47E-02
Ccnd2	ENSMUSG00000000184.12	1.27	6.91E-04
Sfn	ENSMUSG00000047281.3	1.20	3.64E-02
Tspyl2	ENSMUSG00000041096.13	1.15	1.91E-02
Mxd4	ENSMUSG00000037235.13	0.99	1.98E-03
Tgfb1	ENSMUSG00000002603.15	0.94	2.73E-04
Rap2b	ENSMUSG00000036894.3	0.94	3.76E-02
Casp1	ENSMUSG00000025888.6	0.92	6.29E-02
Mxd1	ENSMUSG00000001156.9	0.87	6.10E-02
Btg2	ENSMUSG00000020423.6	0.86	4.83E-03
Cd82	ENSMUSG00000027215.13	0.78	7.13E-02
Epha2	ENSMUSG00000006445.3	0.75	1.33E-02
Hras	ENSMUSG00000025499.18	0.75	3.48E-02
Gm2a	ENSMUSG00000000594.7	0.71	4.16E-02
Iscu	ENSMUSG00000025825.12	0.67	3.42E-03
Tap1	ENSMUSG00000037321.17	0.65	7.15E-02

Rab40c	ENSMUSG00000025730.14	0.65	8.02E-02
Rchy1	ENSMUSG00000029397.15	0.60	4.65E-02
Def6	ENSMUSG00000002257.8	0.50	7.87E-02
Fam162a	ENSMUSG00000003955.8	-0.66	1.03E-03
Steap3	ENSMUSG00000026389.16	-0.69	1.37E-02
Cdkn1a	ENSMUSG00000023067.14	-0.71	8.43E-02
Hint1	ENSMUSG00000020267.6	-0.81	1.73E-04
Rpl36	ENSMUSG00000057863.6	-0.97	2.21E-06
Rps27l	ENSMUSG00000036781.13	-0.98	2.82E-04
Tprkb	ENSMUSG00000054226.13	-1.01	6.27E-04
H2aj	ENSMUSG00000060032.6	-1.08	1.28E-05
Sdc1	ENSMUSG00000020592.14	-1.08	8.63E-02
Rpl18	ENSMUSG00000059070.16	-1.09	1.82E-05
Mknk2	ENSMUSG00000020190.13	-1.09	4.31E-05
H1f2	ENSMUSG00000036181.2	-1.13	3.05E-05
Pcna	ENSMUSG00000027342.14	-1.20	1.41E-07
Ada	ENSMUSG00000017697.3	-1.28	9.91E-05
Pmm1	ENSMUSG00000022474.15	-1.40	1.26E-05
Rack1	ENSMUSG00000020372.15	-1.46	2.33E-08
Rps12	ENSMUSG00000061983.7	-1.58	5.27E-12

padj, Benjamini-Hochberg adjusted p-value

Supplementary Table S2. Flow cytometric antibodies.

Target	Conjugate	Clone	Company	Cat. No.
CD19	APC-Cy7	1D3	BD Biosciences	557655
	FITC	1D3	Biolegend	152404
	eFluor 450	eBIO1D3	eBioscience	48-0193
B220 (CD45R)	PerCP-Cy5.5	RA3-6B2	BD Biosciences	552771
	APC-eFluor780	RA3-6B2	eBioscience	47-0452
CD43	PE	S7	BD Biosciences	553271
CD3	Pacific Blue	17A2	BioLegend	100214
	APC-eFluor780	17A2	eBioscience	47-0032
CD11b	APC-Cy7	M1/70	BD Biosciences	557657
BP-1 (CD249)	Biotin	6C3	eBioscience	13-5891
Streptavidin	APC-Cy7		Biolegend	405208
	eFluor 450		eBioscience	48-4317
	Brilliant Violet 650		Biolegend	405231
IgM	FITC	II/41	eBioscience	11-5790
	Biotin	II/41	eBioscience	13-5790
IgD	APC	11-26	eBioscience	17-5993
Ter119	APC-eFluor 780		eBioscience	47-5921
Ly-6G/Ly-6C (Gr-1)	APC-Cy7	RB6-8C5	Biolegend	108424
	APC-eFluor780	RB6-8C5	eBioscience	47-5931
CD48	PE	HM48-1	eBioscience	12-0481
CD150	Brilliant Violet 510	TC15-12F12.2	Biolegend	115929
CD34	FITC	RAM34	BD Biosciences	553733
CD135	Biotin	A2F10	Biolegend	135308
Sca-1 (Ly6A/E)	PE-Cy7	D7	BD Pharmingen	558162
c-kit (CD117)	PE-Cyanine5	2B8	eBioscience	15-1171
CD127	eFluor 450	A7R34	eBioscience	48-1271

Supplementary Table S3. Immunoblotting antibodies.

Target	Cat. No.	Company
HSC70 (B-6)	sc-7298	Santa Cruz
Cyclin C	A301-989A	Bethyl
CDK8 (G398)	#4101	Cell Signaling
CDK19	HPA007053	Sigma-Aldrich
p53	sc-393031	Santa Cruz
p21	sc-6246	Santa Cruz
p16INK4a	ab211542	Abcam
p19ARF	ab80	Abcam
Cyclin D2	sc-593	Santa Cruz
NDRG1	26902-1-AP	Proteintech
PLK2	15956-1-AP	Proteintech
GADD45a	#4632	Cell Signaling
14-3-3 Sigma	10622-1-AP	Proteintech/Thermo Fisher
Anti-mouse IgG, HRP-linked	#7076	Cell Signaling
Anti-rabbit IgG, HRP-linked	#7074	Cell Signaling

Supplementary Table S4. qRT-PCR primers.

Gene	Forward (5'>3')	Reverse (5'>3')
Actb	CTCTGGCTCCTAGCACCATGAAGA	GTAAAACGCAGCTCAGTAACAGTCCG
Rplp0	GCTTTCTGGAGGGTGTCC	GCTTCAGCTTTGGCAGGG
Cdkn2b	CCCTGCCACCCTTACCAGA	CAGATACCTCGCAATGTCACG
Cdkn1a	GAACATCTCAGGGCCGAAA	ATCTGCGCTTGGAGTGATAG
Gadd45a	CTGCAGAGCAGAAGACCGAA	GGGTCTACGTTGAGCAGCTT
Plk2	GAGCCTCCTTCCGGACAAAA	GAGCCGAGGTCTTCGAATGT
Sfn	TCTGATCCAGAAGGCCAAGT	CCCACCACGTTCTTGTAAGC

Supplementary References

1. Bellutti F, Tigan AS, Nebenfuehr S, et al. CDK6 antagonizes P53-induced responses during tumorigenesis. Cancer Discov 2018;8(7):884–897.

2. Hardy RR. B-cell commitment: Deciding on the players. Curr Opin Immunol 2003;15(2):158–165.

3. Hardy RR, Li Y-S, Allman D, Asano M, Gui M, Hayakawa K. B-cell commitment, development and selection. Immunol Rev 2000;175(1):23–32.

4. Rolink A, Melchers F. Molecular and cellular origins of B lymphocyte diversity. Cell 1991;66(6):1081–1094.

5. Li N, Fassl A, Chick J, et al. Cyclin C is a haploinsufficient tumour suppressor. Nat Cell Biol 2014;16(11):1080–1091.

6. Georgiades P, Ogilvy S, Duval H, et al. VavCre transgenic mice: a tool for mutagenesis in hematopoietic and endothelial lineages. Genesis 2002;34(4):251–256.

7. Kühn R, Schwenk F, Aguet M, Rajewsky K. Inducible gene targeting in mice. Science 1995;269(5229):1427–1429.

8. Schuster C, Berger A, Hoelzl MA, et al. The cooperating mutation or "second hit" determines the immunologic visibility toward MYC-induced murine lymphomas. Blood 2011;118(17):4635–4645.

9. Shaulian E, Zauberman A, Ginsberg D, Oren M. Identification of a Minimal Transforming Domain of p53: Negative Dominance through Abrogation of Sequence-Specific DNA Binding. Mol Cell Biol 1992;12(12):5581–5592.

10. Sexl V, Piekorz R, Moriggl R, et al. Stat5a/b contribute to interleukin 7-induced B-cell precursor expansion, but abl- and bcr/abl-induced transformation are independent of Stat5. Blood 2000;96(6):2277–2283.

11. Hagemann-Jensen M, Ziegenhain C, Chen P, et al. Single-cell RNA counting at allele and isoform resolution using Smart-seq3. Nat Biotechnol 2020 386 2020;38(6):708–714.

12. Bolger AM, Lohse M, Usadel B. Trimmomatic: a flexible trimmer for Illumina sequence data. Bioinformatics 2014;30(15):2114–2120.

13. Smith T, Heger A, Sudbery I. UMI-tools: modeling sequencing errors in Unique Molecular

Identifiers to improve quantification accuracy. Genome Res 2017;27(3):491–499.

14. Frankish A, Diekhans M, Ferreira AM, et al. GENCODE reference annotation for the human and mouse genomes. Nucleic Acids Res 2019;47(D1):D766–D773.

15. Dobin A, Davis CA, Schlesinger F, et al. STAR: ultrafast universal RNA-seq aligner. Bioinformatics 2013;29(1):15–21.

16. Liao Y, Smyth GK, Shi W. featureCounts: an efficient general purpose program for assigning sequence reads to genomic features. Bioinformatics 2014;30(7):923–930.

17. Liao Y, Smyth GK, Shi W. The Subread aligner: Fast, accurate and scalable read mapping by seed-and-vote. Nucleic Acids Res 2013;41(10):e108.

18. R Core Team. R: A Language and Environment for Statistical Computing. *R Foundation for Statistical Computing, Vienna, Austria.*

19. RStudio Team. RStudio: Integrated Development Environment for R (RStudio, PBC, Boston, MA). 2020;URL:http://www.rstudio.com.

20. Love MI, Huber W, Anders S. Moderated estimation of fold change and dispersion for RNA-seq data with DESeq2. Genome Biol 2014;15(12):1–21.

21. Subramanian A, Tamayo P, Mootha VK, et al. Gene set enrichment analysis: A knowledge-based approach for interpreting genome-wide expression profiles. Proc Natl Acad Sci U S A 2005;102(43):15545–15550.

22. Mootha VK, Lindgren CM, Eriksson KF, et al. PGC-1α-responsive genes involved in oxidative phosphorylation are coordinately downregulated in human diabetes. Nat Genet 2003;34(3):267–273.

23. Liberzon A, Subramanian A, Pinchback R, Thorvaldsdóttir H, Tamayo P, Mesirov JP. Molecular signatures database (MSigDB) 3.0. Bioinformatics 2011;27(12):1739–1740.

24. Liberzon A, Birger C, Thorvaldsdóttir H, Ghandi M, Mesirov JP, Tamayo P. The Molecular Signatures Database (MSigDB) hallmark gene set collection. Cell Syst 2015;1(6):417.

25. Meyers RM, Bryan JG, McFarland JM, et al. Computational correction of copy number effect improves specificity of CRISPR-Cas9 essentiality screens in cancer cells. Nat Genet 2017;49(12):1779–1784.

26. Dempster JM, Boyle I, Vazquez F, et al. Chronos: a cell population dynamics model of CRISPR experiments that improves inference of gene fitness effects. Genome Biol 2021;22(1):1–23.

27. Pacini C, Dempster JM, Boyle I, et al. Integrated cross-study datasets of genetic dependencies in cancer. Nat Commun 2021;12(1):1–14.

28. Dempster JM, Rossen J, Kazachkova M, et al. Extracting Biological Insights from the Project Achilles Genome-Scale CRISPR Screens in Cancer Cell Lines. bioRxiv 2019;720243.

29. Ghetti S, Burigotto M, Mattivi A, et al. CRISPR/Cas9 ribonucleoprotein-mediated knockin generation in hTERT-RPE1 cells. STAR Protoc 2021;2(2):100407.

30. Castanza AS, Recla JM, Eby D, Thorvaldsdóttir H, Bult CJ, Mesirov JP. Extending support for mouse data in the Molecular Signatures Database (MSigDB). Nat Methods 2023;20(11):1619–1620.

31. Howe DG, Blake JA, Bradford YM, et al. Model organism data evolving in support of translational medicine. Lab Anim (NY) 2018;47(10):277–289.